

# Radio Subcarrier Multiplexing in Conjunction with Optical Mode Division Multiplexing for 5G Networks

Angela Amphawan, Baseem Khalaf  
School of Computing,  
University Utara Malaysia,  
Sintok, Kedah, Malaysia.  
[angela.amphawan.dr@ieee.org](mailto:angela.amphawan.dr@ieee.org)

Wanasiah Tahir, Hafiza Haron, Rukhiyah Adnan  
Department of Computer Science,  
Kolej Poly-Tech MARA, Cheras,  
Kuala Lumpur, Malaysia

**Abstract**— 5G is speculated to transform the mobile communications landscape by increasing data rates, latency, coverage and energy efficiency. Radio-over-fiber (RoF) provides a high-capacity, efficient and scalable 5G architecture for transporting radio signals through optical fibers, exploiting the enormous bandwidth of the optical fiber cables. In this paper, a new radio-over-fiber (RoF) architecture for future 5G networks is proposed using SCM-MDM for converging data streams from different picocells. Different sets of the Hermite-Gaussian (HG) modes are introduced for the SCM-MDM system in RoF. The effect of different sets of HG modes on the RoF system performance are compared in terms of the transverse electric fields, eye diagrams, modal analyses and bit-error rates. A total throughput of 19.5 Gb/s is achieved.

**Keywords** – 5G, radio-over-fiber (RoF), subcarrier multiplexing (SCM), mode division multiplexing (MDM), Hermite-Gaussian (HG) modes

## Introduction

4G networks are growing exponentially with more networks operators around the world adopting the Long-Term Evolution (LTE) standard [1]. The number of 4G connections globally is projected to rise 18-fold to three billion by 2019 [2]. The escalating traffic growth has motivated the communications industry to look at new architectures which are qualified to handle future vast capacity and performance requirements. Unlike 4G, which is built on a standardized radio access technology LTE, 5G highlights the improvement of current used techniques to optimize data capacity [3]. 5G is speculated to transform mobility landscape. Increased data rates, latency, coverage and energy efficiency are envisioned [4-6] although thus far, standards are still being explored [7].

In light of the above 5G QoS requirements, particularly in terms of data rates and frequency reuse, radio-over-fiber (RoF) provides a high-capacity, efficient and scalable architecture for transporting radio frequency (RF) signals through optical fibers, exploiting the enormous bandwidth of the optical fiber cables. Many wireless network applications have recently adopted RoF to enhance the network performance and

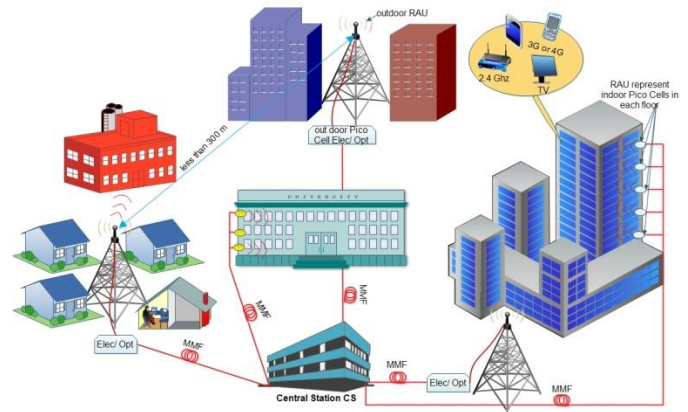


Fig. 1 Distributed antenna system (DAS) based on radio-over-fiber (RoF)

flexibility [8, 9]. One of the adopted applications is the distributed antenna system (DAS). In a DAS, RoF transmission links are utilized to connect a central station (CS) to a group of remote antenna units (RAUs) to provide excellent coverage and exclusive capacity for short-range communications in picocells located offices, malls and airports and other high-traffic areas. Fig. 1 illustrates the DAS principle in a university campus, where the CU and the base stations are co-located in a central building, and RoF links are utilized to connect the RAUs with the CS within the coverage space. The RAUs are distributed in the streets or inside building. Transmitting the collected radio signals from different BSs to CS over an optical link instead of radio links has many benefits:

- Reduces the number of complicated network equipment in the base stations (cost effective)
- Reduces the high electrical power required for cooling system.
- Reduces the latency or time required for signal processing within the base station, all the traffic will be processed in CS
- Efficiently exploits the frequency bands. By reducing the channels required for the backhaul links

Picocells are 10 to 100 times less in cost and more power efficient than 4G current cells (macro cells). The cell cost consideration in 5G is more critical than 4G due to high densities of BSs and increased bandwidth [6].

To multiplex radio frequency (RF) subcarriers from several picocells, optical subcarrier multiplexing (SCM) is typically used. Microwave devices are more mature than optical devices for cellular communications thus allowing ease of integration with current RF systems. The convergence between radio multiplexing schemes and optical multiplexing schemes when has introduced new horizons regarding the mobility of the wireless and wide band of the optical fiber. Sub-carrier multiplexing – Wave Division Multiplexing (SCM-WDM) convergence was implemented in a passive optical network (PON), achieving 10Gb/s [10][11].

The main contribution of this work is to demonstrate an alternative approach for combining several radio subcarriers from different picocells in a DAS using mode division multiplexing (MDM). MDM is a recent technique that allows many propagation modes in MMF to be independently excited, permitting parallel transmission of data streams [12, 13]. MDM has garnered significant attention in optical communications [14-19] but is still unexploited in RoF systems. Utilizing MDM in the context of a DAS allows the RF channels of several antennas to be propagated into a single mode, then converged with more RF channels from further picocells without interference. This is a significant transformation in its own right.

In this paper, we introduce SCM-MDM for RoF using three new sets of Hermite-Gaussian (HG) modes. The performance of MDM relies upon modal selectivity and intermodal dispersion, for maximizing the bandwidth distance product for each channel. Thus, the performance analysis for our proposed SCM-MDM system in RoF will include the investigation of the transverse electric fields, eye diagrams, modal analyses and bit-error rates.

### Methodology

The design and simulation of the proposed SCM-MDM system in RoF was conducted on OptiSystem platform [20] as shown in Fig. 2. The proposed model consists of the radio and optical domains, which work complementarily to achieve SCM-MDM. The radio part of the system adopts SCM for multiplexing several radio subcarriers from different picocells. On the other hand, the optical part will adopt MDM for converging several sets radio subcarriers from different locations through a single multimode fiber (MMF). In addition to the high bandwidth viable through MDM, MDM also effectively reduces the effect of modal dispersion by confining the propagation constants of each channel.

Nine independent data streams were subcarrier multiplexed onto three sets of radio subcarriers at 500MHz, 1000MHz and

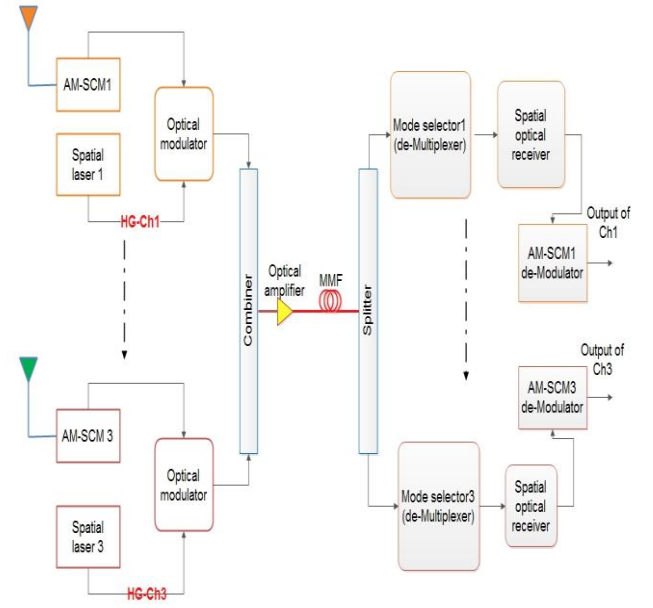


Fig. 2 RoF SCM-MDM design

1500 MHz, each set amplitude modulated (AMed) at a center frequency of 5260 Hz, 5760 MHz and 5825MHz respectively with a gain of 10 dB. The 5GHz is unlicensed and suitable for WLAN applications. The nine SCM amplitude-modulated radio subcarriers were modulated using three Mach-Zander optical modulators with extinction ratio of 30 dB at 6.5 Gb/s driven by three spatial continuous wave (CW) lasers at a wavelength 850 nm. The lasers generate four different sets of HG modes as independent channels to achieve mode division multiplexing. The electric fields of the Hermite-Gaussian modes,  $H_{lm}$  are described by [20]

$$\psi_{lm}(r, \phi) = H_l \left( \frac{\sqrt{2}x}{\omega_{ox}} \right) \exp \left( -\frac{x^2}{\omega_{ox}^2} \right) \exp \left( j \frac{\pi x^2}{\lambda R_{ox}} \right) \times H_m \left( \frac{\sqrt{2}y}{\omega_{oy}} \right) \exp \left( -\frac{y^2}{\omega_{oy}^2} \right) \exp \left( j \frac{\pi y^2}{\lambda R_{oy}} \right) \quad (8)$$

where  $l$  and  $m$  represent mode dependencies on the X and Y-axis.  $R$  is the radius of curvature and  $\omega$  is the spot size.  $H_l$  and  $H_m$  are the Hermite polynomials. Several combinations of HG modes were tested for SCM-MDM in a RoF system.

The modulated optical signals were then be amplified with an optical amplifier of 20 dBm before being coupled into a 300m-long parabolic multimode fiber with a peak refractive index profile of 1.4142. De-multiplexing of HG modes were achieved by noninterferometric mode selection [21] by which the corresponding LP fiber modes with higher power coupling coefficient values were selected and then detected by the spatial

photo detector. The electrical signal was band-pass filtered before AM demodulation to recover the transmitted signal.

### results

Trials of different combinations of HG modes demonstrate that three groups of HG modes were the most effective for propagation of independent radio subcarriers for SCM-MDM, namely:

- (a) Set 1:  $HG_{02}, HG_{21}, H_{11}$
- (b) Set 2:  $HG_{01}, HG_{02}, H_{32}$
- (c) Set 3:  $HG_{22}, HG_{10}, H_{11}$

The above HG modes were selected while preserving all other parameters and system components. The performance of the three sets of HG modes were compared and evaluated in terms of the intensity of the transverse electric field, power coupling coefficient, eye diagram and eye opening and Q-factor.

Fig. 3 shows the intensity of the transverse electric field for different sets of HG modes before being coupled into a MMF and after propagation through a MMF. The intensity fields show that the incident HG modes generated by the spatial continuous wave (CW) laser excited the summation of LP fiber modes which were the closest in geometry to the incident HG modes. This is the most discernable in Fig. 3(c) and Fig. 3(d). The fields demonstrate that mode coupling affects the propagation of modes.

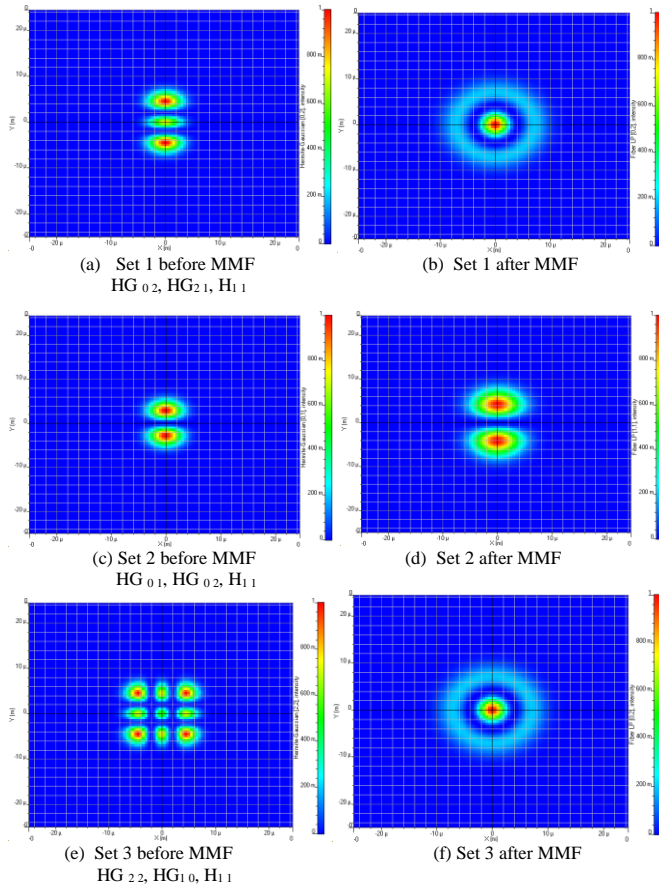


Fig. 3 Intensity of transverse electric fields before and after propagation through MMF

Fig. 4 shows the power coupling coefficient versus modal delay of the different sets of HG modes. Both Set 1 and Set 2 have a Gaussian profile but Set 1 has a shorter pulse width. The pulse width for Set 1 is  $1.415181 \times 10^{-6}$  s, while  $1.415187 \times 10^{-6}$  s for the Set 2, and for Set 3 is  $1.415189 \times 10^{-6}$  s.

Fig. 5 illustrate the eye diagrams, eye height, Q-Factor and BER values at the receiver. Set 1 ( $HG_{02}, HG_{21}, H_{11}$ ) exhibits the lowest BER of  $2.5 \times 10^{-31}$ , highest Q-Factor of 11.58, and highest eye-height of  $5.9 \times 10^{-4}$ , followed by set 2 ( $HG_{01}, HG_{02}, H_{32}$ ) exhibits BER of  $3 \times 10^{-19}$ , Q-Factor of 8.88, and eye height  $6.14 \times 10^{-5}$ , while set 3 ( $HG_{22}, HG_{10}, H_{11}$ ) show BER of  $5.2 \times 10^{-16}$ , Q-Factor of 8, and eye height  $3.5 \times 10^{-4}$ . Comparisons on the BER, Q-Factor, and eye-height for all channels and sets of modes conclude that Set 1 is the most robust.

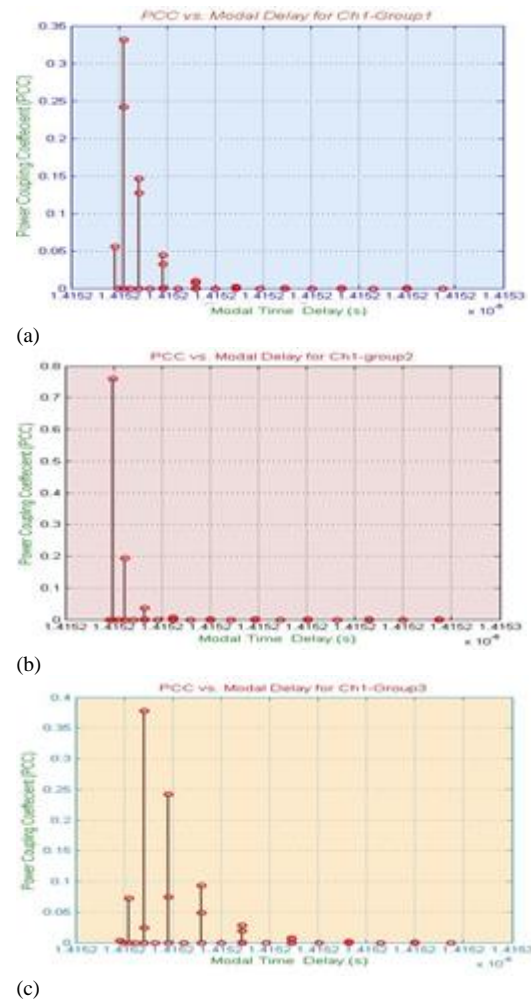


Fig. 4 Power coupling coefficient versus modal delay for Channel 1 for different sets of HG modes: (a) Set 1:  $HG_{02}, HG_{21}, H_{11}$ . (b) Set 2:  $HG_{01}, HG_{02}, H_{32}$ . (c) Set 3:  $HG_{22}, HG_{10}, H_{11}$ .



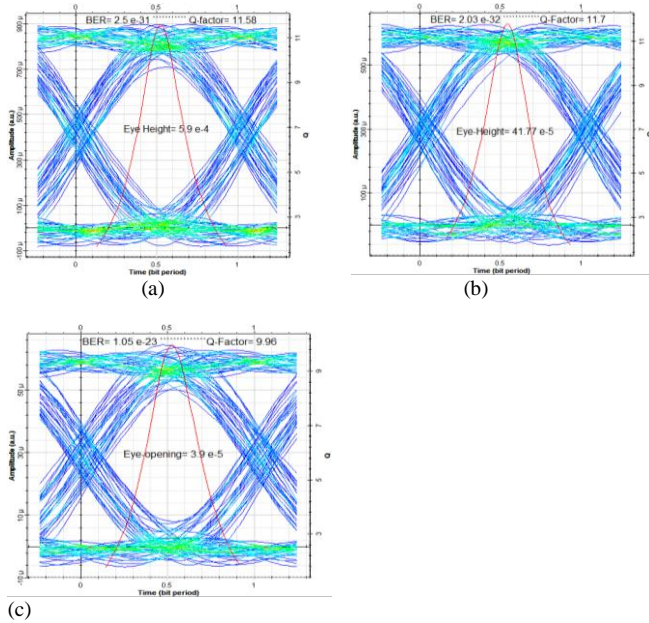


Fig. 5 eye diagrams, eye height, Q-Factor and BER values at the receiver for Channel 1 in different sets of HG modes: (a) Set 1 (b) Set 2 (c) Set 3

### conclusion

A new model for SCM-MDM in a RoF system has been presented comprising three sets of HG modes as independent data carriers at a data rate of 19.5Gb/s through a MMF link of 300m between picocells. Investigation of the power coupling coefficients, BER, Q-Factor, eye height demonstrate that Set 1 comprising HG modes  $HG_{02}$ ,  $HG_{21}$ ,  $H_{11}$  is the most robust, followed by Set 2 and Set 3.

### References

- [1] B. Bangerter, S. Talwar, R. Arefi, and K. Stewart, "Intel," *Communications Magazine, IEEE*, vol. 52, pp. 90-96, 2014.
- [2] Cisco, "Cisco Visual Networking Index: Forecast and Methodology, 2009-2014," San Jose, California 3 Feb. 2015 2015.
- [3] P. K. Agyapong, M. Iwamura, D. Staehle, W. Kiess, and A. Benjebbour, "Design considerations for a 5G network architecture," *Communications Magazine, IEEE*, vol. 52, pp. 65-75, 2014.
- [4] A. Imran, A. Zoha, and A. Abu-Dayya, "Challenges in 5G: how to empower SON with big data for enabling 5G," *Network, IEEE*, vol. 28, pp. 27-33, 2014.
- [5] S. F. Yunas and M. Valkama, "Spectral and energy efficiency of ultra-dense networks under different deployment strategies," *Communications Magazine, IEEE*, vol. 53, pp. 90-100, 2015.
- [6] L. Saker, G. Micallef, S.-E. Elayoubi, and H. O. Scheck, "Impact of picocells on the capacity and energy efficiency of mobile networks," *annals of telecommunications-Annales des télécommunications*, vol. 67, pp. 133-146, 2012.
- [7] W. H. Chin, Z. Fan, and R. Haines, "Emerging technologies and research challenges for 5G wireless networks," *Wireless Communications, IEEE*, vol. 21, pp. 106-112, 2014.
- [8] P. Demestichas, A. Georgakopoulos, D. Karvounas, K. Tsagkaris, V. Stavroulaki, J. Lu, *et al.*, "5G on the horizon: key challenges for the radio-access network," *Vehicular Technology Magazine, IEEE*, vol. 8, pp. 47-53, 2013.
- [9] G. S. Gordon, M. J. Crisp, R. V. Pent, T. D. Wilkinson, and I. H. White, "Feasibility Demonstration of a Mode-Division Multiplexed MIMO-Enabled Radio-Over-Fiber Distributed Antenna System," *Journal of Lightwave Technology*, vol. 32, pp. 3521-3528, 2014.
- [10] R. Gaur, A. Singhal, and K. Pahwa, "Review Paper on Multifarious Optical Networks Differentiated on the basis of various Multiple Access Techniques Techniques."
- [11] D. V. Plant, Z. A. El-Sahn, J. M. Buset, and B. J. Shastri, "Overlapped Subcarrier Multiplexed WDM PONs Enabled by Burst-Mode Receivers," in *Access Networks and In-house Communications*, 2011, p. ATuA3.
- [12] G. S. Gordon, J. Carpenter, M. J. Crisp, T. D. Wilkinson, R. V. Pent, and I. H. White, "Demonstration of radio-over-fibre transmission of broadband MIMO over multimode fibre using mode division multiplexing," in *European Conference and Exhibition on Optical Communication*, 2012, p. Th. 1. B. 1.
- [13] A. Amphawan, "Review of optical multiple-input-multiple-output techniques in multimode fiber," *Optical Engineering*, vol. 50, p. 102001, 2011.
- [14] J. Carpenter, B. C. Thomsen, and T. D. Wilkinson, "Degenerate mode-group division multiplexing," *J. Lightwave Technol.*, vol. 30, pp. 3946-3952, 2012.
- [15] J. Carpenter and T. D. Wilkinson, "Precise modal excitation in multimode fibre for control of modal dispersion and mode-group division multiplexing," in *European Conf. and Exposition on Optical Communications (ECOC)*, Geneva, 2011, p. We.10.P1.
- [16] S. O. Arik and J. M. Kahn, "Adaptive MIMO Signal Processing in Mode-Division Multiplexing," in *Photon. Soc. Summer Topical Meeting Series, 2014 IEEE*, 2014, pp. 192-193.
- [17] A. Amphawan, "Holographic mode-selective launch for bandwidth enhancement in multimode fiber," *Optics Exp.*, vol. 19, pp. 9056-9065, 2011.
- [18] A. Amphawan, "Binary encoded computer generated holograms for temporal phase shifting," *Optics Exp.*, vol. 19, pp. 23085-23096, 2011.
- [19] A. Amphawan, "Binary spatial amplitude modulation of continuous transverse modal electric field using a single lens for mode selectivity in multimode fiber," *J. Mod. Opt.*, vol. 59, pp. 460-469, 2012.
- [20] Optiwave, "Optisystem," ed. Ottawa, Canada, 2014.
- [21] A. Amphawan and D. O'Brien, "Modal Decomposition of Output Field from Holographic Mode Field Generation in a Multimode Fiber Channel," in *IEEE Int. Conf. on Photon. 2010 (ICP2010)*, Langkawi, 2010, pp. 1-5.